# Optimized Vortex Tube Bundle for Large Flow Rate Applications

by

Ruijin Cang

A Thesis Presented in Partial Fulfillment
of the Requirements for the Degree
Master of Science

Approved April 2013 by the
Graduate Supervisory Committee:

Kangping Chen, Chair
Hueiping Huang
Ronald Calhoun

ARIZONA STATE UNIVERSITY

May 2013

ABSTRACT

A vortex tube is a device of a simple structure with no moving parts that can be used to separate a compressed gas into a hot stream and a cold stream. Many studies have been carried out to find the mechanisms of the energy separation in the vortex tube. Recent rapid development in computational fluid dynamics is providing a powerful tool to investigate the complex flow in the vortex tube. However various issues in these numerical simulations remain, such as choosing the most suitable turbulent model, as well as the lack of systematic comparative analysis. LES model for the vortex tube simulation is hardly used in the present literatures, and the influence of parameters on the performance of the vortex tube has scarcely been studied.

This study is aimed to find the influence of various parameters on the performance of the vortex tube, the best geometric value of vortex tube and the realizable method to reach the required cold out flow rate 40 kg/s . First of all, setting up an original 3-D simulation vortex tube model. By comparing experiment results reported in the literature and our simulation results, a most suitable model for the simulation of the vortex tube is obtained. Secondly, simulations are performed to optimize parameters that can deliver a set of desired output, such as cold stream pressure, temperature and flow-rate. The use of the cold air flow for petroleum engineering applications has also been discussed.

Key words: vortex tube; 3-D numerical simulation; parameter optimization

ACKNOWLEDGEMENTS

My most sincere appreciation and gratitude go to my committee chair and advisor, Dr. Kangping Chen, for his never-ending patience, guidance, inspiring mentorship and support in my professional life. Without his help this work would not have been possible. I would like to thank Dr. Hueiping Huang and Dr. Ronald Calhoun, for their time serving as part of my committee.

I would also like to thank students in the group—Jing Yuan, Di Shen. They have been great colleagues to work with and have always been willing to discuss and offer advice on my ideas.

# Table of Contents

CHAPTER Page

CHAPTER Page

# CHAPTER 1

## INTRODUCTION

In certain engineering applications such as gas drilling, the use of a high flow-rate air with high pressure and low temperature can improve process effecicency. In these applications, demand for the cold air stream as high as 40 kg/s is not uncommon. In this thesis, the use of a vortex tube bundle for generating this large flow-rate of cold air stream is proposed and evaluated, using numerical simulations.

Vortex tube is a mechanical device with no moving parts that can separate a compressed gas into a hot and a cold stream (Fig. 1). Pressurized gas is injected tangentially into a swirl chamber and accelerated to a high rate of rotation. This gas motion creates a cold core and a hot shell. Because of a conical nozzle placed at the end of the tube, only the outer hot shell of the compressed gas is allowed to escape from that end (the hot end). The remainder of the cold core gas is forced to return in an inner vortex of reduced diameter within the outer vortex with the same rotational direction to the outer free vortex, which exits through the cold end. Vortex tube has attracted much attention from many scholars and engineers since the discovery of its energy separation effect by the French engineer Ranque in 1930. This is mainly due to vortex tube's light structure, low cost to manufacture and stable operation. Vortex tube has already been used in areas such as refrigeration, aviation, and biopharmaceutical, with potential for even wider applications.

A single commercially available vortex tube can only produce a cold air stream up to 0.008 kg/s. Thus it will take 5,000 such vortex tubes to reach the required flow-

rate of 40 kg/s. Space limitation as well as assemly difficulty makes such an approach unrealistic. The objective of this work is to design a custom-made vortex tube so that a minimum number of such tubes can be used to meet the performance requirement posted by these applications. Table 1.1 summarizes the requirements and the design objectives of this work. Assume the air input from the air compressor to the vortex tube is at a temperature of 20$^{o}$C. The "Temperature Drop" in the table refers to the temperature difference between the air entering the vortex tube and the exiting cold air stream from the vortex tube, while the "Required Pressure" refers to the cold stream pressure.

Table 1.1 Design requirements

| Required Total Flow Rate | Required Pressure | Temperature Drop | Number of Tubes |
|---|---|---|---|
| 40 kg/s | 2.5 MPa | as high as possible | as few as possible |

The flow in a vortex tube involves very complicated heat transfer and fluid flow, and there is still no unified theory that can explain the energy separation mechanism convincingly. In this study, computational fluid dynamics is used to analyze the flow field, temperature field and pressure field, and to optimize the vortex tube parameters so that a specific set of desired output can be achieved to meet the application requirement specified in Table 1.1.

### 1. 1 Background

The history of the vortex tube can be traced back to 1930. While making a tornado device which would be used to separate gas from mineral, French metallurgical engineer G.J. Ranque found a very interesting phenomenon that the

temperature in the central portion of the gas in the cyclone separator was lower than that at the outer part. This came to known as the vortex energy separation effect, or simply energy (or temperature) separation effect.

Ranque published the first paper on the temperature separation effect in the vortex tube in 1931, and he also filed a patent successfully in France. In 1932, he filed the patent again in the U.S. and it was approved in 1934 [1]. In 1933, Ranque presented a research report about the vortex tube and the temperature separation effect at the French Physics Association [2]. In the report, the two vortex tube structures in his patent were shown, which contained downstream and countercurrent vortex tube. He also showed designs of different number of inlets with various shapes. The report pointed out that when compressible air with temperature of 20$^{o}$C entered the inlet of a vortex tube, the temperature of the air came out from the cold outlet could reach -10$^{o}$C to -20$^{o}$C, while the hot end stream could be 35$^{o}$C. However, when he tried to explain this phenomenon, he miss-understood the concept of total temperature and static temperature, which caused many scholars to refuse to recognize his achievement. Because of this ordeal, such a significant finding was put aside for the next twelve years.

In 1945, an American scientist came to visit German university Erlangen, and re-discovered the use of vortex tube. The physicist Hilsch did a lot of research and finally published a paper [3] that drew new attention to the vortex tube in 1947. In the paper, comprehensive materials were put forward to prove the existence of temperature separation, and Hilsch also offered some constructive suggestions about the parameters, the device settings, and applications of the vortex tube. Hilsch believed that every part of the vortex tube has an optimal ratio between them; the temperature drop has something to do with pressure increase; when the pressure ratio

is fixed at a certain value, the larger the radius of the tube, the better the performance of the vortex tube; the cold outlet should be close to the inlet in order to have a larger temperature drop, and when the ratio of the cold outlet radius to the main tube radius is between 0.45 and 0.60, it gives better results for the temperature drop. All of these guidelines are still being used in the practice even today. Hilsch also pointed out that the efficiency of the vortex tube is very low, and he predicted that the vortex tube usage may be limited by this low efficiency. Because of the research of Hilsch, the world has recognized the practical value of vortex tube. To commemorate Ranque and Hilsch, the vortex tube is also called the Ranque-Hilsch tube, and the effect of the temperature separation is called the Ranque-Hilsch effect.

Normally, a vortex tube is assembled by nozzle, swirl chamber, cold end tube and hot end tube. Fig. 1 shows the air flow process in a vortex tube: the air expands at the inlet of the tube; it then enters the swirl chamber with a high tangential velocity. The air then travels towards the hot end of the vortex tube, and separates into two parts, hot air at the outside and cold air in the middle. Once reached the conical valve, the cold air travels backward and flows out through the cold outlet; and the hot air flows out through the hot outlet. The ratio of the cold air to the hot air can be adjusted via the conical valve at the hot end in order to have the best performance of the vortex tube.

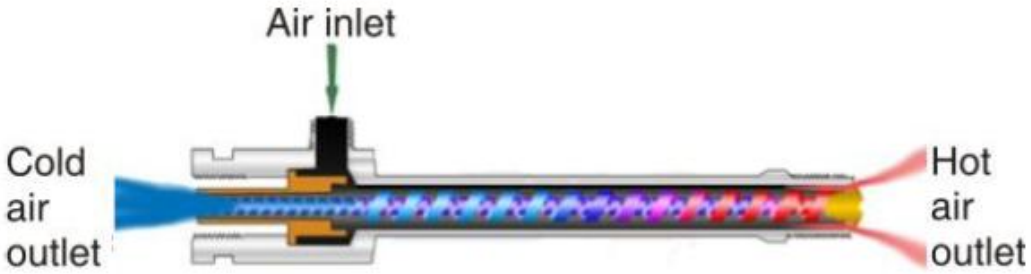


Fig. 1. Schematic drawing of a vortex tube operational mechanism [58]

Vortex tube offers many advantages [4]:

(a) Safe and reliable; easy to be installed and removed; and no Freon is needed.

(b) Compact structure, light and low cost.

(c) No rotating parts; long working time with no maintenance.

(d) Only air is needed, abundantly available with no pollution.

(e) Can be made by stainless steel, anti-corrosion and longevity.

With so many advantages, vortex tube attracts researchers from the world [49]. Large companies such as Shell Oil Exploration Company, Fulton Hypothermia, Baike Flight Company，Hanike Flight Company and Philip Oil Company all have patents on vortex tube, varying from theory, experiment, to fields of applications. Meanwhile, companies focus on manufacturing vortex tube also emerged, such as Vortex, Exxair and Transonic in the US.

So far vortex tube is widely used in the following fields [50]:

(1) Machining: Bearing Cooling, Chip Processing Cooling, Solidify hot melt, small air conditioner [5][6] and vortex tube type heat exchanger [7].

(2) Scientific Research: Thermostat of thermocouple cold junction, whirlpool thermostat, temperature calibration, materials testing, thermal expansion test and etc.

(3) Biomedical: Biological freezing, surgery and etc.

(4) Aviation Technology: the scroll adjustment device of aviation spacecraft, cooling of electronic device, De-icing[8].

(5) Petrochemical Industry: Natural gas cooling, separation and liquefaction [9-16,51].

Vortex tube is not without shortcomings. It has at least two important disadvantages: it has a limited flow-rate: it cannot be applied to operations requiring a large flow-rate. This is the problem I am trying to over-come in the present study. The second issue is low efficiency, which was predicted by Hilsch. However, in some situations, efficiency is not the only economic indicator to measure the benefits of using a vortex tube [9-16]. For example, for a small system or an intermittent motion device, it is more economical to use portable, tight, reliable, cheap vortex tubes than using a high efficiency, complicated cooling system. Thus, optimizing the design of a vortex tube to meet specific needs that efficiency is a secondary consideration is of practical interests to certain applications.

### 1.2 Literature Review

Research on vortex tube has been carried out based on theory, experiment, and numerical simulation. The goal of a theoretical study is to find the physical mechanisms of the temperature separation effect, and put forward a mathematical model that describes truthfully the underlying physics. Experiment is used to validate theory and to analyze the parameters for the optimized design of the vortex tube. Numerical simulation computes approximate flow field and can be used to carry out virtual experiments. Numerical simulation is the method of choice for the present study.

### 1.2.1 Review of Vortex Tube theory

Although vortex tube has a simple structure and it is easy to manipulate, its inner energy exchange is very complicated. Because of the existence of friction between the flows, the heat transfer process is irreversible, and the flow in the tube is a three dimensional compressible turbulent flow. At this time, there is no single mathematical model that can predict the performance of the vortex tube very well. Explanation of the effect of temperature separation has drawn divergent views, none of which is completely satisfying, and some of them are even conflicting with each other. Certain consensus, however, have been reached:

(a) In the same tube, at any fixed cross-section, the static pressure is the highest near the wall and lowest near the axis;

(b) In the same tube, at any fixed cross-section, the temperature is the highest near the wall and lowest near the axis;

(c) Tangential velocity plays as a key role;

(d) When compressed air leaves the compressor nozzle and enters the tube, the flow field can be divided into two parts, one is a free vortex moving towards the hot outlet at the outer region, formed by air rotating along the tangential direction of the tube wall; and a counter-flowing forced vortex in the center of the tube turned back by the conical valve at the hot outlet. In any tube cross-section, the total temperature is always the highest near the wall and lowest near the axis. The highest total temperature along the axis is at the hot end outlet, and the lowest is at the cold end outlet.

The pressure, velocity and temperature distribution in a vortex tube can be studied using the conservation laws for mass, momentum and energy. The following is

a summary of the results from the literature:

(1) Vortex momentum transfer theory

Fulton [11] was the first to analyze the temperature separation effect of a vortex tube. He believed that, in the process of forming the free vortex, kinetic energy exchange occurs in the radial direction, which induces a temperature gradient along the radial direction. Based on this conjecture, Fulton derived a relationship between the temperature difference at both of the hot end and the cold end and the turbulence Prandtl number:

$$\frac{\Delta T_{c,max}}{\Delta T} = 1 - \frac{1}{2P_r} \qquad (1.1)$$

where $\Delta T_{c,max}$ is the maximum temperature drop from the inlet temperature, which occurs at the cold outlet; $\Delta T$ is the temperature difference between the hot end and the cold end; and Pr is the Prandtl number, defined by the ratio between viscosity diffusion rate v and thermal diffusion rate α.

Van Deemter [12] provided a generalized Bernoulli equation to analyze the vortex tube temperature separation mechanism. He pointed out that there is a kinetic energy exchange from the axis to the tube wall, which was consistent with Fulton's view [11].

Webster [52] and Lay [13] analyzed the flow of the free and the forced vortex, and proposed fluid viscous effect as an important factor for the energy separation. They believed that the high-speed rotation fluid layer in the vortex tube has friction caused by viscosity, which makes the kinetic energy to transfer from the axis to the wall, and the energy separation thus occurs.

(2) Theory of expansion work

Based on the analysis of the three dimensional energy equation, Deissler and Perlmutter [15] think that the key factor of energy separation of vortex tube is the fluid compressibility: a compressible fluid must expand in order to cool the fluid. The turbulence shear power between the forced vortex in the central part of the tube and free vortex at outer layer makes the largest contribution to the temperature separation effect. Turbulence shear power can be divided into a diffusion term, a kinetic energy term and a pressure term. In the free vortex layer, the total temperature rises because of the diffusion term. However, in the central forced vortex zone, the total temperature drops because of the kinetic energy term and the pressure term.

(3) Theory of acoustic streaming

Kurosaka [22] puts forward a very unique proposition: he believes that the acoustic movement caused by orderly disturbance in the vortex tube is the reason for the occurrence of energy separation effect. After the high speed airflow entering vortex tube, helix traveling wave is formed in the tube, which stimulates Stokes wave near the tube wall, then the Stokes wave stimulate acoustic wave, and finally causing the resonance of acoustic wave, making the Ranque vortex with small vortex core becomes a rotating solid type of forced vortex filled in the tube (except the boundary layer), which causing the radial separation of temperature. He mentions that if one installs muffler in the vortex tube with downstream structure, adjusting the basic tangential wave to discrete frequency, with smaller amplitudes, then the temperature separation effect will be weaken.

Eckert [23] also published a paper in 1986, considering coupled effect of the pressure and wave. According to the noise produced by vortex tube, known as “vortex howling”, he believed that the airflow in the tube is oscillatory in nature. Thus, when the sound intensity is increased, the effect of energy separation is enhanced. He

mentions that the energy separation effect is produced by the pressure on the pulsating wave-like flow lines, while the viscosity plays a supporting role. This theory is becoming more and more accretive to researchers in the field.

### 1.2.2 Review of Experiment on Vortex Tube

In the 1931 patent of Ranque's, he pointed that the vortex tube could be of two types, the downstream type and counter flow type. Downstream type means outer layer hot flow flows out through hot end outlet, while the middle cold flow flows out through the cold end in the opposite direction. In the counter flow type, both hot and cold air flows out through the hot end. It has been proved through experiments that the efficiency of the counter flow type vortex tube is only half as much as downstream flow type. Thus, the downstream flow type vortex tube is normally used. Figure 1.2 is an example of downstream type vortex tube [28].


Fig. 1.2 basic components of vortex tube [60]

There are lots of parameters that can affect the vortex tube performance. A tree diagram of these parameters is listed below:

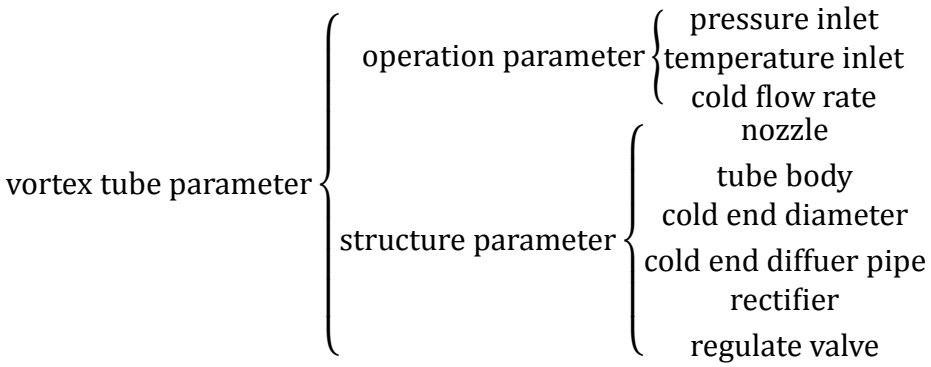


Before discussing the influence of different parameters, simple descriptions about the performance of vortex tube characterizing parameters are listed below:

Refrigeration effect of vortex tube: $\Delta T_c = T_0 - T_c$ ;

Heating effect of vortex tube: $\Delta T_h = T_0 - T_c$ ;

Vortex tube cold flow rate ratio: $\mu = \frac{m_c}{m_0}$ ;

vortex tube unit cooling capacity: $q=\mu \cdot C_p \cdot \Delta T_c$ ;

vortex tube refrigeration efficiency: $COP=\frac{q}{RT_0 \ln(\frac{p_0}{p_c})}$

In the above:

$T_0$ ----- vortex tube inlet temperature, K;

$T_c$ ----- vortex tube cold end temperature, K;

$T_h$ ----- vortex tube hot end temperature, K;

$p_0$ ---- vortex tube inlet pressure, Pa;

$p_c$ ---- vortex tube cold end pressure, Pa;

$p_h$ ---- vortex tube hot end pressure, Pa;

$m_0$ ---- vortex tube inlet mass flow rate, kg/s;

$m_c$ ---- vortex tube cold end mass flow rate, kg/s;

$m_h$----vortex tube hot end mass flow rate, kg/s;

(1) Operation parameters

- inlet pressure $p_0$: Inlet pressure is a key parameter influencing the performance of vortex tube [31-35]. Most of the articles uses expansion ratio $\varepsilon$ , defined as the pressure ratio between the inlet and the cold end outlet:

$$\varepsilon = p_0/p_c \qquad (1.7)$$

to characterize the inlet pressure effect. In most of experimental studies, the pressure at the cold end outlet is fixed at the local atmospheric pressure. There are, however, several works using variable pressure at the cold end outlet. Studies on the inlet pressure shows that the energy separation effect increases with the inlet pressure, but levels off to a constant at very high inlet pressures. Thus, as the inlet pressure is increased higher and higher, the rate of increases in the pay-off becomes smaller, which may not justify the use of very high inlet pressure.

- inlet temperature $T_0$: there are fewer articles on the inlet temperature effect because it is not easy to adjust and maintain the inlet temperature. From the limited number of experiments in the literature and my simulation to be discussed below, it is shown that the inlet temperature has limited effect on the vortex tube performance.

(2) Structural parameters

- nozzle: this is a very important part of a vortex tube. After an extensive review of literature, I believe that the structure of nozzle can be characterized by several aspects:

(a) intake: there are helical intake and tangential intake. Takahama and Parulekar etc believe tangential intake is better than the other type [48-50].

(b) the form of the nozzle: it means that the cross section of the inlet. The usual forms include straight nozzle, tapered nozzle. From experimental data in the literature, which can be found is that, the tapered nozzle provides a better performance than the other one [35,36,48-50].

(c) cross section of nozzle: the usual shape should be round cross section and rectangular cross section. Among the two form, rectangular performs better[35,36,38,42,45,48,51].

(d) number of nozzles: use of different number of nozzles influences the performance as well. The usual numbers are: 1, 2, 3, 4, 5, 6, 8. Among them, 4 and 6 is considered to be better [35,36,38,42,45,48,51].

### 1.2.3 Review of Numerical Simulation on Vortex Tube

Computational Fluid Dynamics is one of the most useful tools for solving complicated flow problems. Because of the complicated coupled flow and heat transfer, there is still no well-accepted model or method for numerical simulation in a vortex tube.

A commonly used turbulence model for vortex tube simulation is Standard k-ε. The model was developed as a 2D steady axisymmetric model. The diameter of the tube is 12mm, the ratio between the tube diameter to length is 10/35, size of cold end diameters are from 5mm to 7.5mm, numbers of inlet nozzle are 1, 2, 6, nozzle shape (asymptote type, straight type and round, rectangular). The boundary condition is,

inlet pressure 0.5422MPa, and inlet temperature is 300K; cold end outlet pressure is 0.136MPa; hot end pressure is changeable according to flow rate. The results are as follows: (1) velocity and temperature distribution------along with the rotation velocity distribution, axial velocity distribution, radial velocity distribution and axial temperature distribution are computed; (2) six inlet nozzles is found to provide the best performance. (3) when the cold end outlet diameter is 6mm, the temperature drop is the largest; (4) the ratio between length and diameter influences the refrigeration effect limitedly. The tube length to tube diameter ratio has a marginal effect on the vortex tube performance. Beheral [34] and Alijuwavhel [54] did the same research and came to the same conclusions.

Bramo [55] employed the standard k-ε model and ideal gas as working fluid in the simulation. Three dimensional grid has been used in the vortex tube model by Exxair company. The results show that the standard k-ε model is better than RNG k-ε model. The standard k-ε model predicts flow and temperature field more accurately: the forced vortex occupies the majority of the tube cross-section, and the percentage of which decreases towards the cold end; energy separation effect happens mainly near the inlet area of the tube, mainly because of the strong pressure gradient at the radial and axial direction.

### 1.3 The Scope of the Current Study

Based on the discussion above, preliminary simulations will be performed for original vortex tube under the conditions carried out in the experiments reported in the literature [56]. Variations of the parameters of the vortex tube will then be studied and compared to the experiments.

Simulations will then be performed to optimize the parameters of the original vortex tube in order to have the best performance of the separation effect.

# CHAPTER 2

# NUMERICAL METHOD, CODE VALIDATION AND VERIFICAION

## 2.1 Numerical Model for Simulation

Skye [56] believes that in order to understand the complicated flow and heat transfer phenomenon of the vortex tube, the velocity, pressure and temperature distributions in the tube needs to be found. The rapid development of computational fluid dynamics (CFD) provides us a convenient and faster way to study on these variables in a vortex tube. As discussed above, because of the complexity of the vortex flow in the tube, choice of a suitable turbulence model is still inconclusive. Here the standard k-ε turbulence model is employed since it has a better performance, as discussed above. The random number generation k-ε turbulence model and more advanced turbulence models such as the Reynolds stress equations and RNG k-ε were also investigated. However it was found that it is harder to achieve convergence results for the cases studied here. Nader [58] showed that, because of good agreement of numerical results with the experimental data, the k-ε model can be selected to simulate the effect of turbulence inside of computational domain. Thus, the k-ε model will be used in all our simulations.

The mass, momentum, and energy conservation equations are:

$$\frac{\partial}{\partial x_j}\left(\rho u_j\right) = 0 \qquad (1)$$

$$\frac{\partial}{\partial x_j}\left(\rho u_i u_j\right) = -\frac{\partial p}{\partial x_i} + \frac{\partial}{\partial x_j}\left[\mu\left(\frac{\partial u_i}{\partial x_j} + \frac{\partial u_j}{\partial x_i} - \frac{2}{3}\delta_{ij}\frac{\partial u_k}{\partial x_k}\right)\right] + \frac{\partial}{\partial x_j}\left(-\bar{\rho}\overline{u_i}'\overline{u_j}'\right) \qquad (2)$$

$$\frac{\partial}{\partial x_j}\left[u_i\rho\left(h + \frac{1}{2}u_j u_j\right)\right] = \frac{\partial}{\partial x_j}\left[k\frac{\partial T}{\partial x_j} + u_i\left(\tau_{ij}\right)\right] \qquad (3)$$

where the $u_j$ is velocity, ρ is density, μ is viscosity coefficient, h is enthalpy and $\tau_{ij}$ is the stress tensor component;

In the present study, the ideal gas equation is used:

$$p = \rho RT \quad (4)$$

The kinetic energy(k) of turbulence and ε (rate of dissipation) are derived from:

$$\frac{\partial}{\partial t}(\rho k) + \frac{\partial}{\partial x_t}(\rho k u_i) = \frac{\partial}{\partial x_j}\left[\left(\mu + \frac{\mu_t}{\sigma_k}\right)\frac{\partial k}{\partial x_j}\right] + G_k + G_b - \rho\epsilon - Y_M \quad (5)$$

$$\frac{\partial}{\partial t}(\rho k) + \frac{\partial}{\partial x_i}(\rho \varepsilon u_i) = \frac{\partial}{\partial x_i}\left[\left(\mu + \frac{\mu_t}{\sigma_\varepsilon}\right)\frac{\partial \epsilon}{\partial x_j}\right] + C_{1\varepsilon}\frac{\varepsilon}{k}(G_k + C_{3\varepsilon}G_b) - C_{2\varepsilon}\rho\frac{\varepsilon^2}{k} \quad (6)$$

In the equations above, $G_k$, $G_b$, and $Y_M$ represent the production of turbulence kinetic energy according to the average velocity gradients, the generation of turbulence kinetic energy according to buoyancy, and the contribution of fluctuating dilatation in compressible turbulence to the overall dissipation rate, respectively. $C_{1\varepsilon}$ and $C_{2\varepsilon}$ are constants. $\sigma_k$and $\sigma_\epsilon$ are the turbulent Prandtl number (Pr) for k and ε. The turbulent ( or eddy) viscosity, $\mu_t$, is computed as:

$$\mu_t = \rho C_\mu \frac{k^2}{\varepsilon} \quad (7)$$

where $C_\mu$ is a constant. The model constants $C_{1\varepsilon}, C_{2\varepsilon}, C_\mu, \sigma_k$and $\sigma_\epsilon$ will be as:

$C_{1\varepsilon} = 1.44, C_{2\varepsilon} = 1.92, C_\mu = 0.09, \sigma_k = 1.0$ and $\sigma_\epsilon = 1.3$.

### 2.2 Geometric Model of Vortex Tube

A picture and schematic of the vortex tube are shown below as Fig. 2.1 and Fig. 2.2. The 10.6 cm working tube length is where the energy separation effect occurs. Also it will be used as the geometry for the CFD model, which will be described in the following chapter.

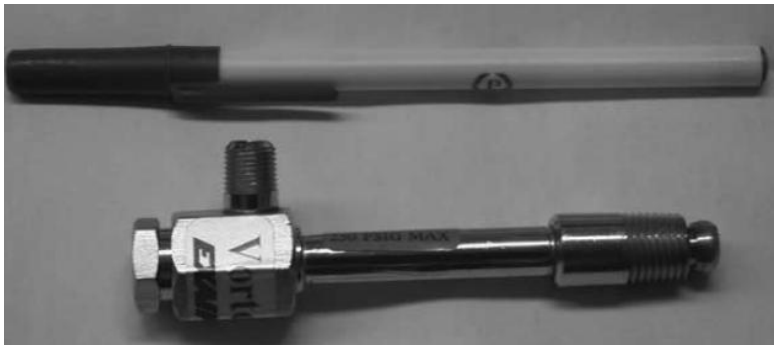

Fig. 2.2 vortex tube [60]

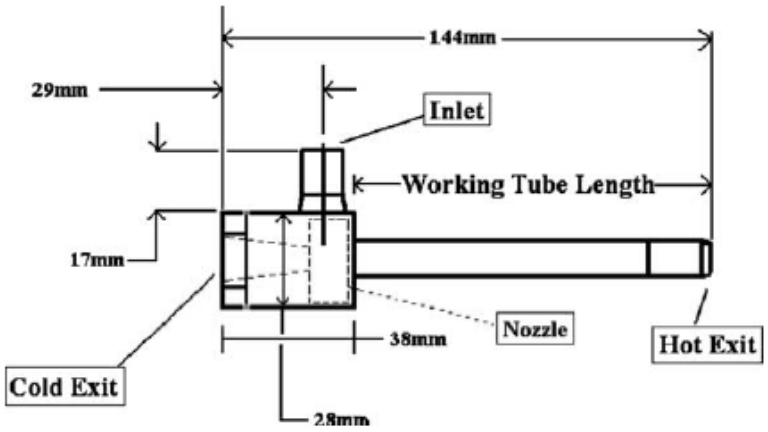


Fig. 2.3 schematic of vortex tube

The cold and hot exits are axial orifices with areas of 30.2 and 95 $mm^2$, respectively, as measured with a micrometer. The nozzle of the vortex tube consists of 1 straight slot that direct the flow to high tangential velocities. The parameter values are listed in the following table.

Table 2.1 Geometric measurements of the vortex tube

| Vortex tube geometry summary | | |
|---|---|---|
| Measurement | Value | Uncertainty |
| Working tube length | 10.6 cm | 0.1 cm |
| Working tube I.D. | 1.14 cm | 0.01 cm |
| Nozzle total inlet area | 8.2 $mm^2$ | 7 % |
| Cold exit diameter | 6.2 mm | 1.4 % |
| Cold exit area | 30.3 $mm^2$ | 3 % |
| Hot exit diameter | 11.0 mm | 0.1 mm |
| Hot exit area | 95 $mm^2$ | 4 % |

The table above describes the basic parameters of the vortex tube, and will be used in our initial simulations in the next Chapter.

### 2.3 Numerical Results and Code Validation

#### 2.3.1 Mesh Generation

Overall, meshing method can be viewed as three ways: structured grid, non-structured grid and half-structured grid. Using structured mesh, the density of meshing can be controlled in any direction; however, such meshing method may not be able to adapt to complicated shape. Non-structured mesh adapts well to complicated shape. It can choose type and topology automatically according to the shape. The operation is easy, but meshing quality is not as good as structured meshing methods. Half-structured meshing is a combination of structured and non-structured meshing method; it uses structured meshing in the area with regular shape, and non-structured meshing in irregular area. Such method has not only good shape adapting ability, but high

meshing quality as well. Normally, numerical computation has the following three requirements for mesh generation: body-fitted, smooth, reasonable density and good orthogonality.

By governing equation, control volume integral method, discrete equation, numerical solution will definitely has some difference to the exact solution, and such difference is mainly called discretization error. The magnititude discretization error has some relation to the truncation error. Under the same grid step, discrete error is getting small along with the increasing rank. To one discrete format, the closer the mesh is the smaller the error is. However, the close level of the mesh depends on the computer itself and limit of rounding errors. Generally, the mesh level of numerical computation satisfies such request: further refinement on the mesh are also employed, the residual doesn't change much, thus results can be believed and trusted.

Grid independence analysis is to check the influence to the result according to the size of the grid. Here one of the representative values in the vortex tube is chosen, temperature drop, to check whether my grid is good for my simulation.

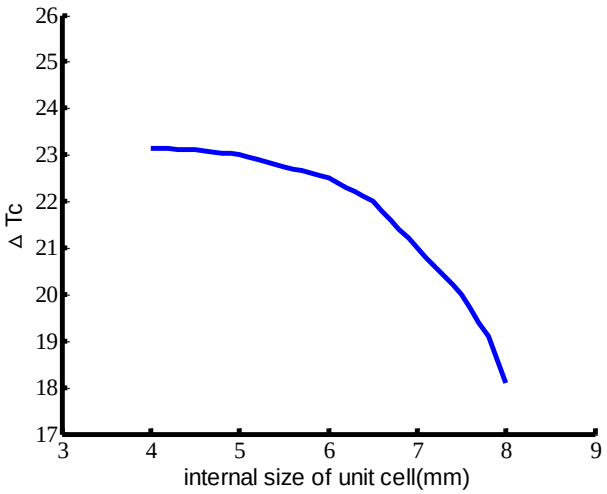


Fig. 2.4 grid independent check

From the figure 2.4 above, as is known that when the size of grid is small than 5mm, the change of the result is very small. So my simulation in this report employs the 5mm hexahedral structural mesh, like the figure 2.5 below.

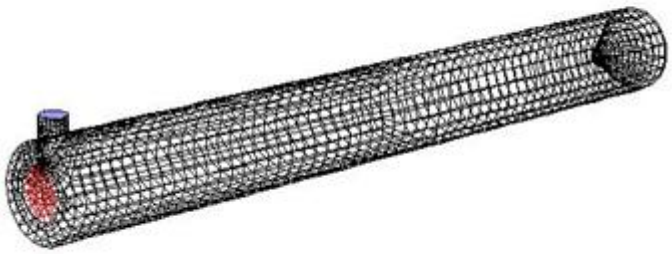

Fig. 2.5 Mesh scheme

### 2.3.2 Boundary Condition

According to Skye's experiment, the boundary condition could be as: inlet nozzle employs as pressure inlet, the pressure sets as 0.4 MPa and the air temperature is 294.2K; outlet employs as pressure outlet and pressure at the cold end outlet can be set as atmospheric pressure; the pressure at the hot end outlet is set as 0.06MPa in order to have a simple comparison to the experiment value.

In Fluent, boundary condition can be set done by two steps, the first one is to preset the boundary condition in meshing section, such as the material type (divided as fluid, solid, porous media) in every sub model, the position of inlet/outlet of the fluid model and its type, the boundary condition of wall and etc; Then just entering the Fluent solver, and go specific boundary conditions parameter settings.

The following simulations are based on the experiment results by Skye. Here are the detail settings:

The gas in the vortex tube is set as ideal-gas.

Set the reference pressure to be 101325 Pa, gravity is not considered.

The inlet of vortex tube is set as pressure-inlet, and the pressure is $P_{in}$ = 4 bar, and the inlet pressure is $T_i$ = 294.2K.

The cold outlet of vortex tube is set as $P_c$ = 0.1 MPa

The hot outlet of vortex tube is set as $P_h$ = 0.06 MPa

The outside wall of vortex tube is set as stationary wall.

Table 2.2 Basic Boundary Condition

| | |
|---|---|
| Fluid type | Ideal-gas |
| Inlet pressure | 0.4MPa |
| Inlet temperature | 294.2K |
| Cold outlet pressure | 0.1MPa |
| Hot outlet pressure | 0.06MPa |
| Wall type | Stationary wall |

The simulation is about three dimensional compressible turbulent flow, and the coupling of fluid and heat transfer is involved in the computation. Based on these conditions, the computation methods can be set as following:

Define>models>solver, solver is selected as three dimensional segregated implicit solver.

Define>models>energy, activate the energy equation.

Define>models>viscous, normally k- ε turbulent model is employed in engineering field.

Solve>controls>solution, the diffusive algorithms of governing equation: pressure option set as standard, pressure-velocity coupling option set as simple

algorithms. Momentum, turbulent kinetic energy, turbulent dissipation rate and energy equation are set as first-order upwind.

Standard of convergence: continuity and the convergence criteria about velocity on x, y, z three directions is 0.001. The convergence criteria of energy equation is 1e-6.

After finishing the above boundary condition and computation methods settings, the numerical simulation begins.

First of all, executing initialization, and then opening the monitor of residuals, and set the convergence standard before the simulation. From the result a phenomenon can be seen is that after about 30,000 iterations, the residuals of different variables reach the convergent standard, which is 1e-5.

### 2.3.3 Simulation Results

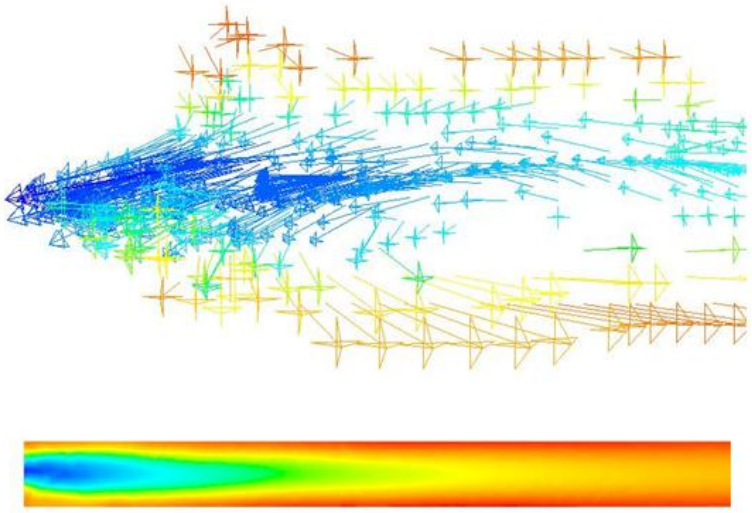

Fig. 2.6 vortex tube cross section velocity vector map

From the Fig. 2.6 above, it can be seen clearly that the air in the tube at the outside zone flow towards the hot end outlet, however, the air in the middle part flow towards the cold end outlet. The energy separation effect can be approved also by the

picture, which is the same to the experiment by Skye.

During the research on vortex tube, it is always expected to know whether the temperature separation really occurs, and what the temperature could the hot-outlet/cold-outlet reach. Thus, first of all, the distribution of temperature in the vortex tube needs to be considered.

In order to have a clear understanding of the temperature distribution and easy to make a comparison to the experiment, here a map is showed, as the figure 2.7

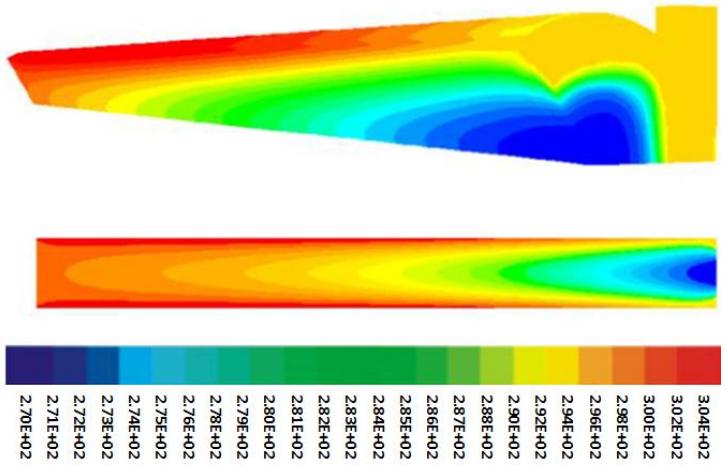


Fig. 2.7 temperature distribution(contour)

It is delightful to know that, it can be seen that the energy separation in the swirl chamber clearly from the picture. Because of the interaction between the inner layer flow and the outer layer flow, the energy inside is decreasing, especially near the middle part, however, the energy is increasing in the outside. So energy separation between the middle part of the tube and the out part does exist, and it can be seen from along the axis peripheral direction, the temperature is increasing. It reaches the highest at the hot-outlet. The temperature at the middle part of vortex tube is lower than the peripheral. It decreases along the axis direction and it reaches the lowest at

the cold-outlet.

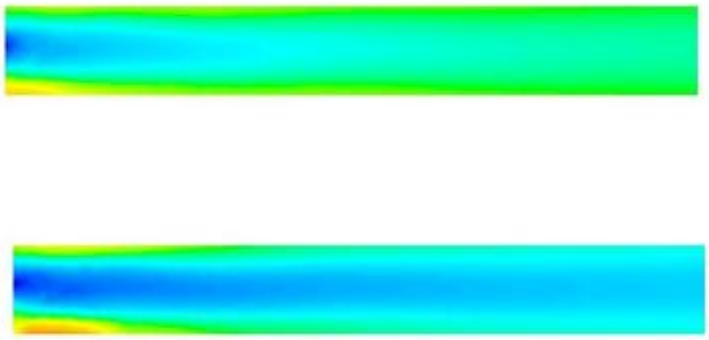

Fig. 2.8 static pressure and total pressure distribution

From above figure 2.8, it can be seen that the distributions of total pressure and static pressure are increasing from the center of the tube to the tube surface, increasing from the cold end to the hot end, which guarantees the air will flow back to the cold end.

### 2.4 comparison between experiment and numerical method

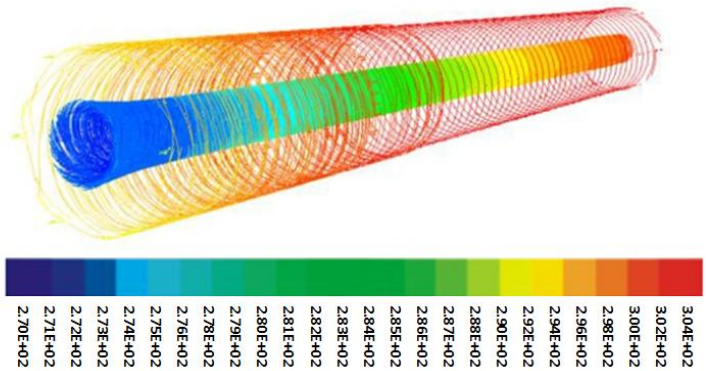


Fig. 2.9 temperature distribution(path line)

From the temperature distribution map Fig. 2.9, it could be seen that the highest

temperature is 304 K at the hot-outlet, and the lowest temperature is 270K at the cold-outlet. Comparing to the air at the inlet nozzle, the hot end rises 8K and the cold end drops 14K, so the total temperature difference is 22. Let's look at Skye's experiment results: The temperature at the hot end is 302K, and the cold end is 274, so the total temperature difference is 28K. The following table 2.3 shows the difference in a clear way.

| | $\Delta T_c$ , $^oC$ | $\Delta T_h$, $^oC$ | Total $\Delta$ T, $^oC$ |
|---|---|---|---|
| CFD method | 24 | 10 | 34 |
| Experiment | 20 | 8 | 28 |

From both of the results, numerical simulation and experiment, because of the simplification made in the simulation process, the result of simulation has some error to the real experiment, but it is still acceptable. Especially, the simulation result shows out the temperature separation effect.

The results of simulation and experiment have some deviation, from the data it can be seen clearly. I believe that such deviations are caused by:

(1) In numerical simulation, the wall function is different from the real wall of the vortex tube;

(2) Some of the parameters in the turbulence model may need to be modified to carry in to the simulation.

(3) The results of experiment itself may have errors, axis velocity and tangential velocity are calculated through pressure and temperature, and however, these two values have measurement error.

From the above simulation, one thing is determined that my results from Fluent are similar to the results by experiment. So here other simulation based on the same

turbulence model and process can be carried to find out other good vortex tube parameters.

# CHAPTER 3

# NEW TUBE DESIGN AND PERFORMANCE EVALUATION

The performance of a vortex tube depends on many parameters as has been mentioned in Chapter 1. The performances are sensitive to some parameters, while insensitive to others. The influences of some parameters are not monotonous, and there should be optimal values that will provide the best result. In this Chapter, a parametric study is carried on to find out such optimal parameter values.

## 3.1 The Operation Parameter Analysis

Parameter optimization is carried out by maintaining constant values for all parameters while varying just a single parameter. In this case, the two important operation parameters are the inlet temperature and the pressure. The geometry of the vortex tube analyzed is the one given in the previous chapter.

### 3.1.1 Vortex Tube Inlet Temperature Optimization Analysis

The figures below show the variation of the inlet temperature on the refrigeration effect, heating effect and flow-rate of the cold stream exiting the cold end. In these calculations, the inlet pressure is fixed at 0.4MPa.

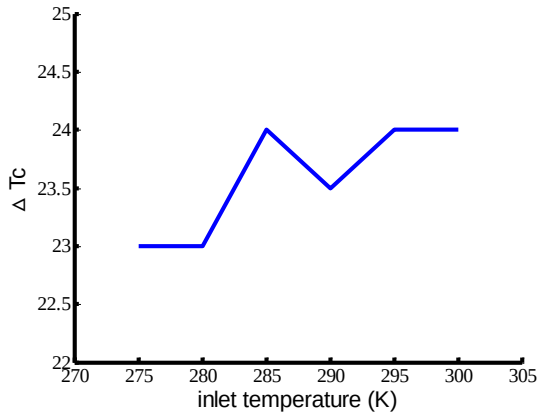


Fig. 3.1 Effect of inlet temperature on the temperature drop from the cold outlet.

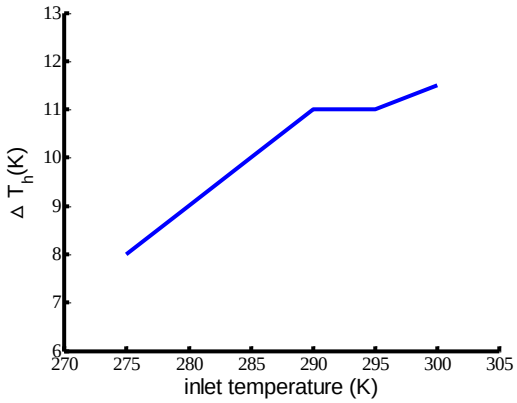


Fig. 3.2 Effect of inlet temperature on the temperature increase from the hot outlet.

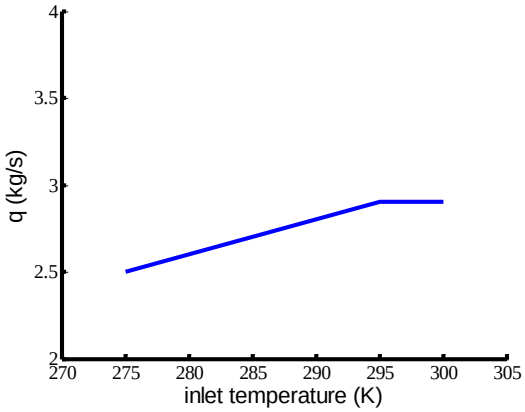


Fig. 3.3 Effect of inlet temperature on the flow rate of the cold stream.

Figures 3.1, 3.2, 3.3 show that the influence of the inlet temperature on the energy separation effect is very small. This is actually good news in some sense, since

no pre-heating or pre-refrigeration is required to achieve the desired energy separation effect.

### 3.1.2 Vortex Tube Inlet Pressure Optimization Analysis

Based on the basic theory of vortex tube, inlet pressure is the key power source making energy separation works. Thus, parametric study on the inlet pressure effect is extremely important.

Using the same method as has been done on the inlet nozzle temperature effect, changing the pressure at the inlet nozzle while keeping other conditions the same. The inlet temperature is fixed at 294.2K. Fig. 3.4 shows the effect of inlet-pressure/cold-outlet-pressure ratio on the temperature drop of the cold air stream (refrigeration effect). As the inlet pressure ratio increases, the expansion ratio of the air goes up, leading to increased temperature drop at the cold end.

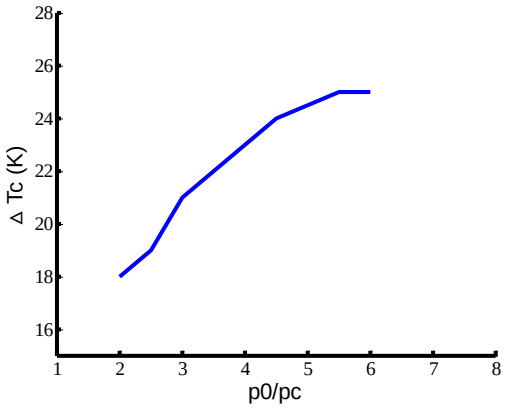


Fig. 3.4 Effect of inlet pressure on the temperature drop at the cold exit.

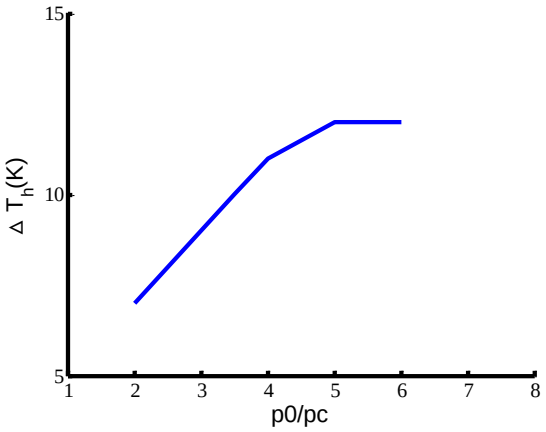


Fig. 3.5 Effect of inlet pressure on temperature rise at the hot exit.

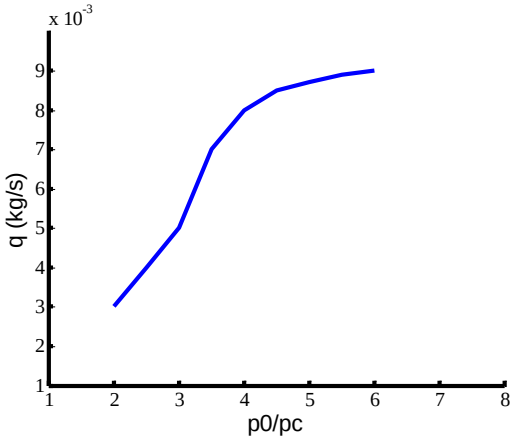


g. 3.6 Effect of inlet pressure on cold stream flow rate.

While not a primary concern, increasing the inlet-pressure/cold-outlet-pressure ratio also benefits the heating effect, as the temperature rise from the hot end also increases (Fig. 3.5). The flow rate of the cold air stream also increases with the pressure ratio (Fig. 3.6).

These results show the benefit of increasing the inlet-to-the-cold-outlet pressure ratio on both refrigeration and heating. The reason for this increase in the performance is due to the increased swirling velocity at the inlet from a higher pressure ratio. As this pressure ratio is increased further, however, the rate of change in the refrigeration and heating eventually levels off as the air speed near the inlet approaches the speed

of sound. Ultimately, when shock waves appear at very large inlet-to-outlet-pressure ratios, the trend actually will be reversed. This dramatic reversal of the pressure ratio effect will be further analyzed below.

The general results of the influence of inlet pressure and inlet temperature on the energy separation effect for the original vortex tube should carry over for any vortex tube. Thus, the general trend will be utilized in the following for designing new vortex tubes.

### 3.2 Simple Modification of the Previous Tube

It has been shown that high pressure at the inlet nozzle will improve the performance of separation effect. In the case of interest to us, however, there are certain requirements on both the temperature drop and the flow-rate of the cold air stream. To this end, it can be observed from the Fig. 3.4-3.6, that when the pressure ratio is 4, the vortex tube can provide a temperature drop of 24 K, and the ratio of the cold stream flow-rate to inlet flow-rate is one-half.

As mentioned in Chapter 1, our task is to deliver a flow-rate of 40 kg/s with a cold end exit pressure of 2.5 MPa. Obviously the vortex tube design described in the previous chapter is not large enough to meet this flow-rate requirement. The most intuitive way to meet the design objective is to simply enlarge the tube described proportionally. This approach should be adopted as a starting point for further optimization by enlarging the original design 10 times geometrically.

Fig. 3.7 shows the temperature distribution along the vortex tube when the inlet pressure is fixed at 8 MPa and the outlet pressure is fixed at 2.5 MPa. These preliminary results indicate that there is still room for further improvements in

performance.

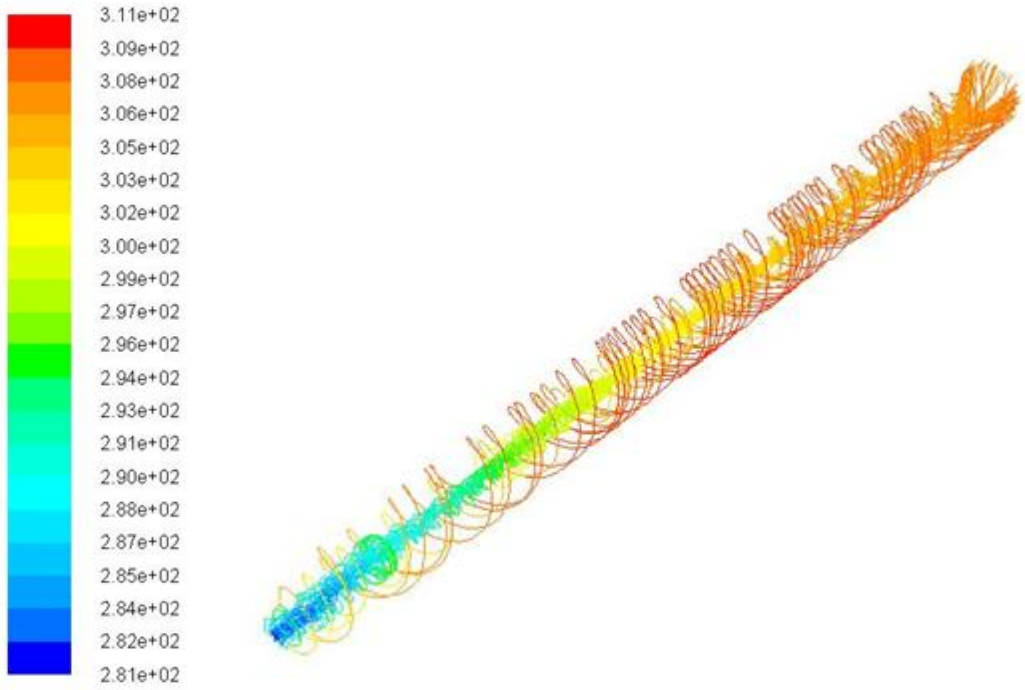


Fig. 3.7 Vortex tube temperature distribution

There are five ways to improve the design by changing: the size of the inlet; the size of the outlets (cold, hot); the diameter of the tube; and the length of the tube. The method adopted here to explore the optimal design is to vary one geometric parameter while maintaining the rest of four geometric parameters constant.

### 3.3 Inlet Parameter Optimization

The inlet is the beginning of the whole tube, and it is chosen to be the first. It has been found that the tangential velocity plays a very important role in the energy separation effect, and the tangential velocity depends on the shape of the inlet pipe. The original vortex tube had a circular inlet, and it was later modified to an elliptical shape by some researchers. It was found that decreasing the minor-to-major semi-axis ratio, called aspect ratio, increases the tangential velocity, thus enhancing the energy

separation effect. Nader [58] mentioned that an aspect ratio of 0.6 delivers a better result than aspect ratio of one (circular inlet). A rectangular inlet pipe has been employed with different aspect ratios for the inlet nozzle, similar to the approach of Upendra [62]. Then the temperature drop at the cold exit can be calculated. These results are shown in Table 3.1.

Table 3.1 Cold exit temperature drop for different Aspect Ratio of rectangular inlet (short/long width)

| AR | $\Delta T_c$, $^oC$ |
|---|---|
| 0.6 | 16 |
| 0.4 | 17 |
| 0.3 | 18 |
| 0.2 | 18 |

From the table above, it is seen that the general trend is that a smaller aspect ratio provides better cooling performance. As the aspect ratio becomes smaller and smaller, however, this improvement seems to level off, with the aspect ratio of 0.2 delivering the best cooling effect.

In addition to the shape of the inlet tube, the cross-sectional area of the inlet tube is also an important parameter. Yu [57] showed that the (inlet-tube area) to the (the vortex tube area) ratio (called “nozzle ratio”) affect the performance of the temperature drop. The effect of different inlet nozzle area on the vortex tube performance is studied while keeping other parameter fixed, for rectangular inlet with aspect ratio of 0.2. Five different inlet areas are investigated, with the results summarized in Table 3.2.

Table 3.2 Effect of inlet area on cold exit temperature drop and flow rate

| S (inlet area), $mm^2$ | $\Delta T_c$, $^oC$ | $q_{in} / q_{cold}$ (inlet-flow-rate/cold-outlet-flow-rate) |
|---|---|---|
| 252.2 | 18 | 1.7 |
| 378.45 | 20 | 2.1 |
| 756.9 | 17 | 2.6 |
| 922.5 | 15 | 3.0 |
| 2000 | 12 | 3.5 |

It is seen from this table, that it is not possible to maximize the cold exit temperature drop and the cold stream flow-rate for the same choice of the inlet area. However, this table provides a good reference for other calculations that intends to perform.

### 3.4 Vortex Tube Cold end Outlet Optimization

Merculov [59] found that there's a range of diameter ratio between cold end outlet orifice to the diameter of the tube, $D_c / D$, between 0.45-0.6, that will optimize the cold stream temperature drop. This diameter ratio will be extended to 0.45 to 0.75, with four cold end outlet orifices. Furthermore, while our previous simulation shows that the inlet to the cold outlet pressure ratio of four provides the best temperature drop when the radius ratio was one, various inlet-to-cold-outlet pressure ratios will be considered in our calculations below for diameter ratios $D_c / D$ between 0.45 and 0.75.

The basic geometric size of the tube for current research is length(L) equals 1024mm, the diameter of the tube(D) is 57mm, the area of inlet($S_{in}$) is 378.45$mm^2$

with the rectangular inlet length h equals 8.7mm and width w=43.5mm, the radius for the outlet-hot is 25mm. So, the only un-determined geometric parameter is the diameter of the cold exit orifice. This value can be chosen as an optimization geometric parameter in the following study.

Now consider a bundle of such tubes. Each of such a tube has the same exit pressure at the cold exit, which is fixed at 2.5MPa. The number of such tubes in the bundle, N, is chosen so that the total flow-rate from the cold exit is 40 kg/s. The only control flow variable is the inlet pressure. Since the flow-rate of the cold stream from a single tube changes with both the inlet pressure and the cold exit orifice diameter, the number of tubes required, N, also changes with the inlet pressure and cold exit orifice diameter.

In Fig. 3.8, the cold-exit-flow-rate vs. the cold exit temperature drop are plotted, with the inlet pressure and the cold exit orifice diameter as parameters. There are four curves in Fig. 3.8, each marked with different colors, corresponding to four cold exit orifice diameter to tube diameter ratios $D_c / D$ of 0.45, 0.55, 0.65, 0.75, respectively. On each of these curves, the cold exit orifice diameter remains the same, the value of which is indicated in the figure legend, and the inlet pressure, $P_{in}$, changes. Thus, the flow-rate of the cold stream, q, as well as the cold stream temperature drop, $\Delta T_c$, also changes along each curve. The number of such tubes required to meet the total cold stream flow-rate, N, at the data point for the curve are also marked.

For any given cold exit orifice diameter, starting with a small inlet pressure, an inlet temperature of 294.2K, while keeping the cold exit pressure at 2.5 MPa. Then gradually increasing the inlet pressure, and compute the cold outlet flow-rate and the cold outlet temperature. As the inlet pressure is increased, the cold air temperature

drops and the inlet flow-rate increases. For example, for $D_c / D = 0.65$ (black color curve), the computation starts with an inlet pressure $p_0 = 5MPa$. What can be found is that the cold stream temperature is $\Delta T_c = 17^0 C$, and 56 tubes (N = 56) are needed to meet the total cold air flow-rate requirement of 40kg/s. As the inlet pressure is increased to $6MPa$, the cold air temperature increases to $\Delta T_c = 19^0 C$, and the N is dramatically reduced to 32. This trend continues as the inlet pressure is further increased, and the curve moves in the direction of increased cold air temperature drop and increased cold air flow-rate (decreased value for N). When the inlet pressure is increased to $8MPa$, however, the cold stream temperature drop reaches its maximum, with $\Delta T_c = 22^0 C$. Beyond this value for the inlet pressure, the cold air temperature drop starts to decrease, while the flow-rate continues to rise. Thus, for any given cold exit diameter, there is an optimal inlet pressure that will give the maximum temperature drop at the cold exit. This optimal inlet pressure actually corresponds to the critical condition for the inlet air: the inlet air Mach number becomes one at this inlet pressure. Beyond this inlet pressure, shock waves appear at the inlet, as will be shown in the next section. Thus, it is preferable to operate in the inlet pressure range where the inlet air is at subsonic speed.

Similar trends are observed for other exit orifice diameters in Fig. 3.8 for Dc/D=0.45,0.55,0.65,0.75. It is also observed that there is an optimal choice for the cold exit orifice diameter as far as the largest temperature drop is concerned: $D_c / D = 0.65$ gives the maximum cold air temperature drop, with inlet pressure of 8MPa, and N = 16. This would represent a reasonable design for a bundle of vortex tube: a $22^0 C$ temperature drop with 16 tubes to meet the total cold air requirement of 40kg/s, and exit pressure of 2.5MPa.

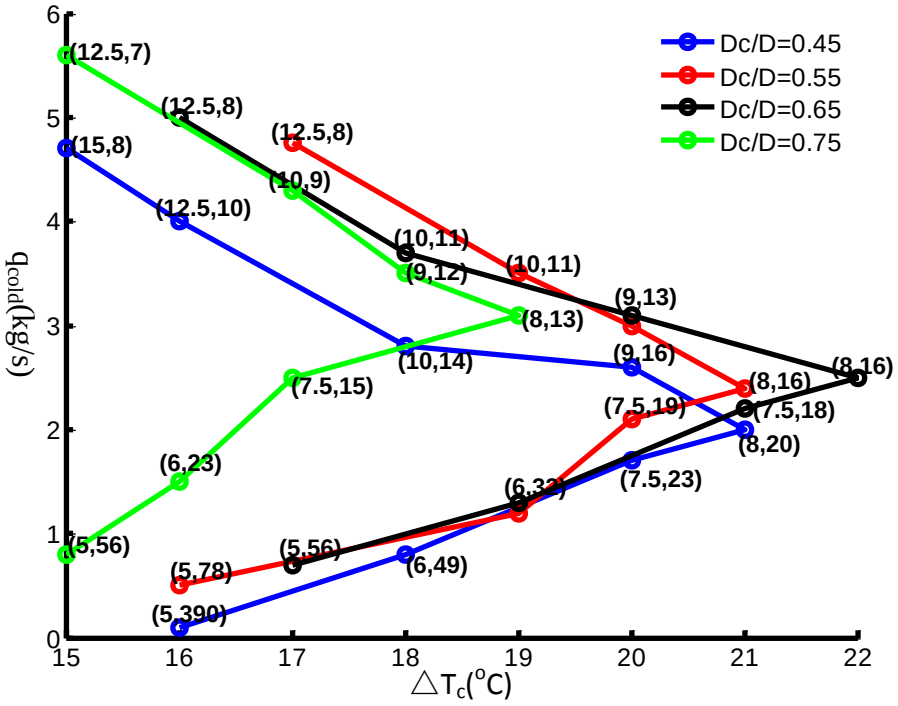


Fig. 3.8 Vortex tube bundle optimization with cold exit orifice diameter and inlet pressure. The (inlet-pressure, number of tubes) pair, ($P_{in}$, N), are marked on each data point along each curve of the same cold exit orifice diameter.

The trend reversal in the curves in Fig. 3.8 can be understood by plotting the Mach number distribution along the vortex tube axis. In Fig. 3.9, such plots for $D_c / D = 0.65$ and various inlet pressures are shown. The inlet tube is located around 0.005m to 0.05m. For any given inlet pressure, the Mach number near the inlet is always the highest. When the inlet pressure is less or equal to 8 MPa, the Mach number along the axis is everywhere below one, indicating subsonic flow in the entire vortex tube. On the other hand, when the inlet pressure is above 9 MPa, the highest Mach number is greater than one, which indicates that shock waves will appear near the inlet. Thus, the reversal in the curves given in Fig. 3.8 corresponds to the subsonic to supersonic flow transition near the inlet. The temperature distribution

along the tube axis for different inlet pressures plotted in Fig. 3.10 clearly shows the non-monotonic variation of the exit temperature with the inlet pressure, confirming the trends shown in Fig. 3.8.

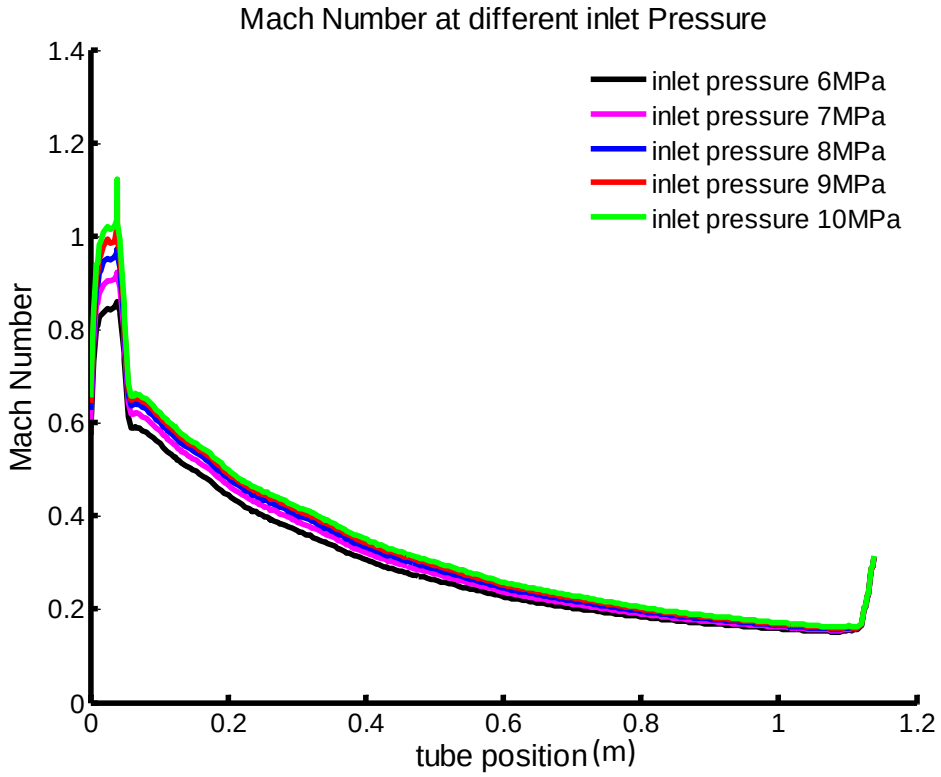


Fig. 3.9 Mach (Ma) number distribution along the tube axis for different inlet pressures. $D_c / D = 0.65$. The inlet to the is located at x = 0.005m to 0.05m

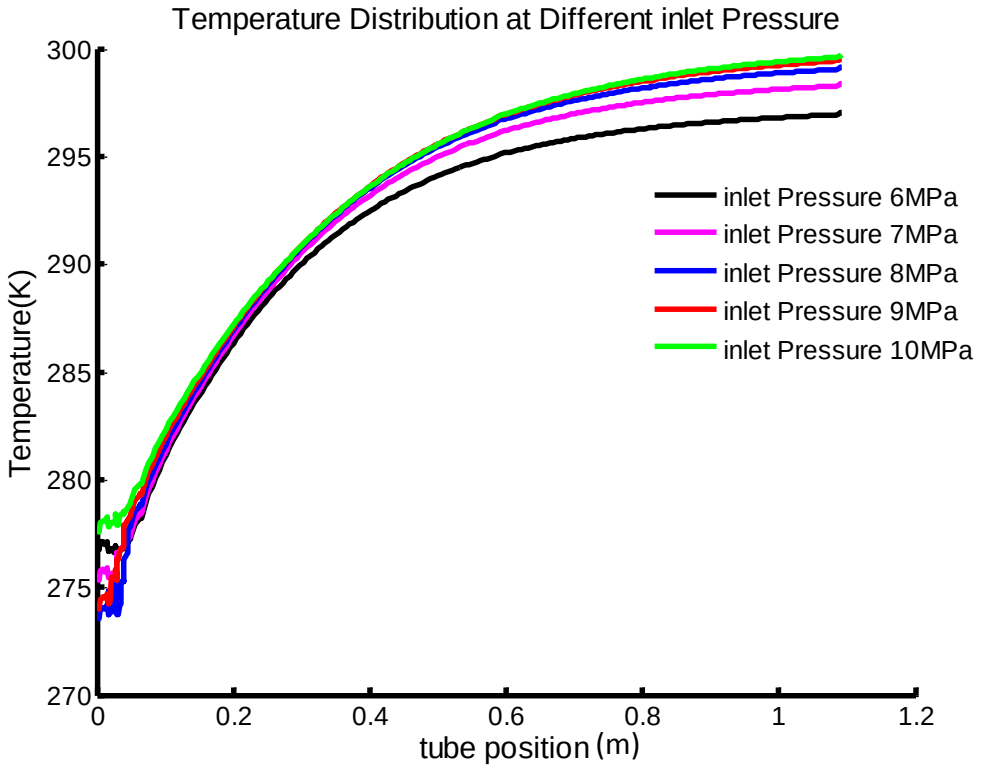


Fig. 3.10 Temperature distribution along the tube axis for different inlet pressures, showing non-monotonic a variant with the inlet pressure, with $D_c / D = 0.65$.

## 3.5 Hot-end Outlet Optimization

### 3.5.1 Shape and Angle

The outlet at hot end has a ring shape. In the original vortex tube, it is movable in order to change the flow rate for different use. However, in our case, it is not that convenient and not necessary to change such area often. So determine a certain size of this area is necessary in order to have the best performance. Several angles and shapes shown in Fig. 3.11 have been used. However, there appears to have no significant difference in the results.

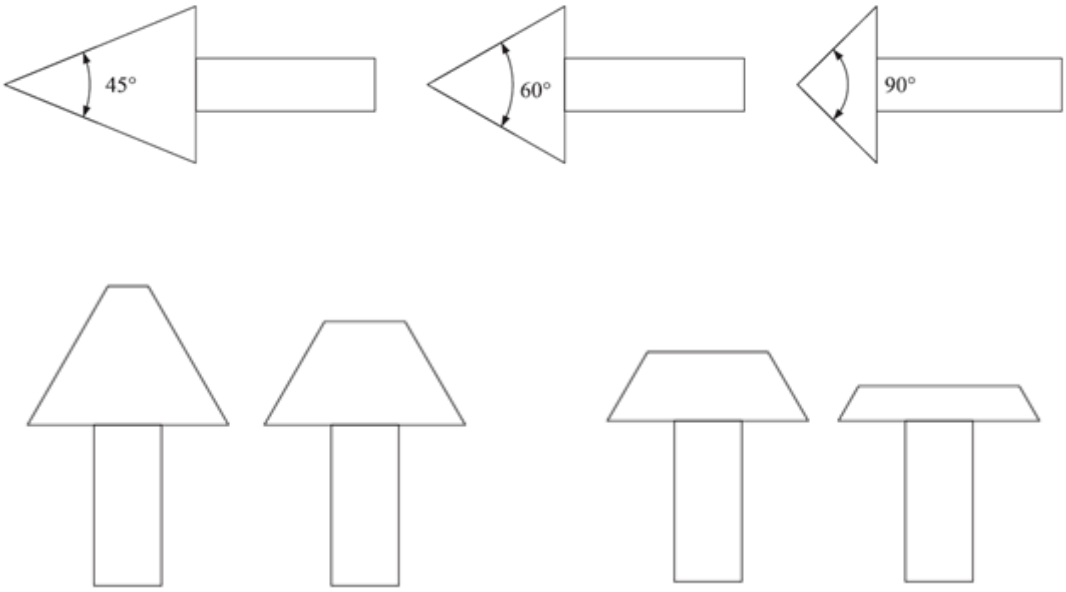


Fig. 3.11 The different shape of hot end outlet

### 3.5.2 The Area of Hot-end Outlet

In addition to the shape and the angle of the hot end valve, the area of the outlet should also be considered. The results are summarized in Table 3.3.

Table 3.3 Effect of hot outlet radius on temperature drop and flow rate

| $R_{hot}$ , cm | $\Delta T_c$ ,$^oC$ | $q_{in}/q_{cold}$ |
|---|---|---|
| 23 | 19 | 2.2 |
| 24 | 21 | 2.3 |
| 25 | 22 | 2.5 |
| 26 | 18 | 2.8 |
| 27 | 17 | 3.2 |

Based on the input value, the inlet pressure is 8MPa and the pressure at the cold end outlet is 2.5MPa, the values of the radius for the hot end outlet can be determined

as 25cm in order to have the best performance.

### 3.6 Length Of the Tube

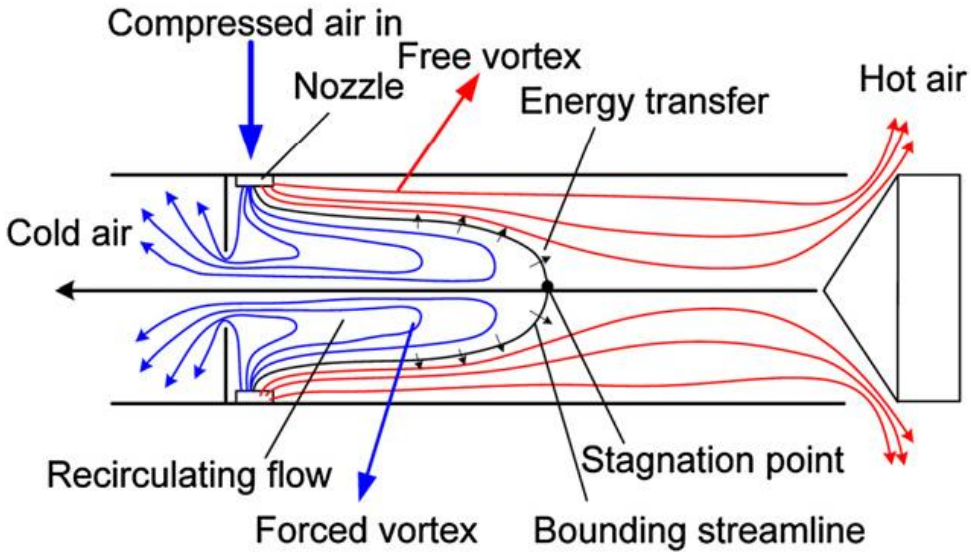


Fig. 3.12 Schematic flow pattern of the tube [57]

Fig. 3.12 shows that as the length of the tube increases, the hot end temperature could be very different. As discussed early, however, the temperature drop of cold air and flow rate are highly concerned about, not the temperature rise of the hot air. Table 3.4 lists our simulation results for tubes with different length. As seen in this table, when the tube reaches certain length, the cold air temperature drop no long increases. A length of 79.8cm gives the largest temperature drop and with the shortest length.

Table 3.4 Temperature drop with different length

| L, cm | Temperature Drop($\Delta T_c$,$^oC$) |
|---|---|
| 136.8 | 22 |

| | |
|---|---|
| 125.4 | 21 |
| 102.6 | 21 |
| 91.2 | 22 |
| 79.8 | 22 |
| 68.4 | 18 |
| 57.0 | 14 |

### 3.7 Geometric Optimization Summary

The optimization process conducted in this Chapter leads to the following optimized set of geometric parameters for a new design of vortex tube that meets our specified requirement:

Table 3.5 Optimized geometric parameters

| | |
|---|---|
| Length of the tube | 798mm |
| Diameter of the tube | 57mm |
| Inlet area of the tube | 378.45mm$^2$ |
| Inlet Rectangular Aspect ratio | 0.2 |
| Inlet nozzle size | h=8.7mm w=43.5mm |
| Radius of hot outlet | 25mm |
| Radius of cold outlet | 14.25mm |

Fig. 3.13 below provides a mesh scheme with the best geometric value as mentioned above.

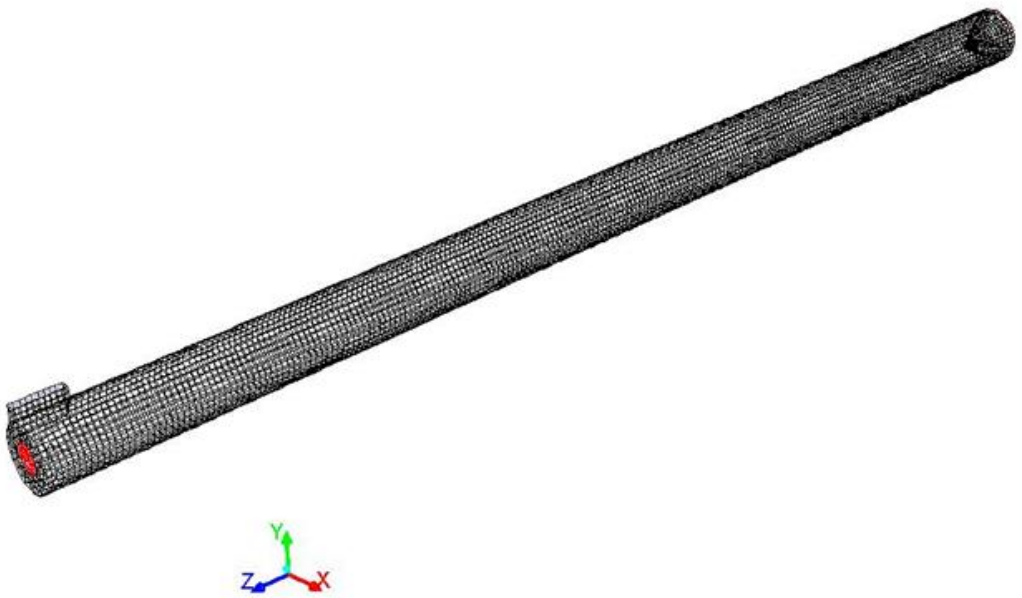


Fig. 3.13 Mesh Scheme

# CHAPTER 4

# AIR DRILLING APPLICATION

## 4.1 Description

The cold air generated by the vortex tube bundle can be used in air drilling operations to cool the drilling bits. To this end, the temperature drop from inlet to the drill pipe to the location of the drilling head at various depths has also been studied, as depicted in Fig. 4.1. The “Outlet 1” marks the location of the drilling head, and “Outlet 2” is the exit of the air with rock pieces.

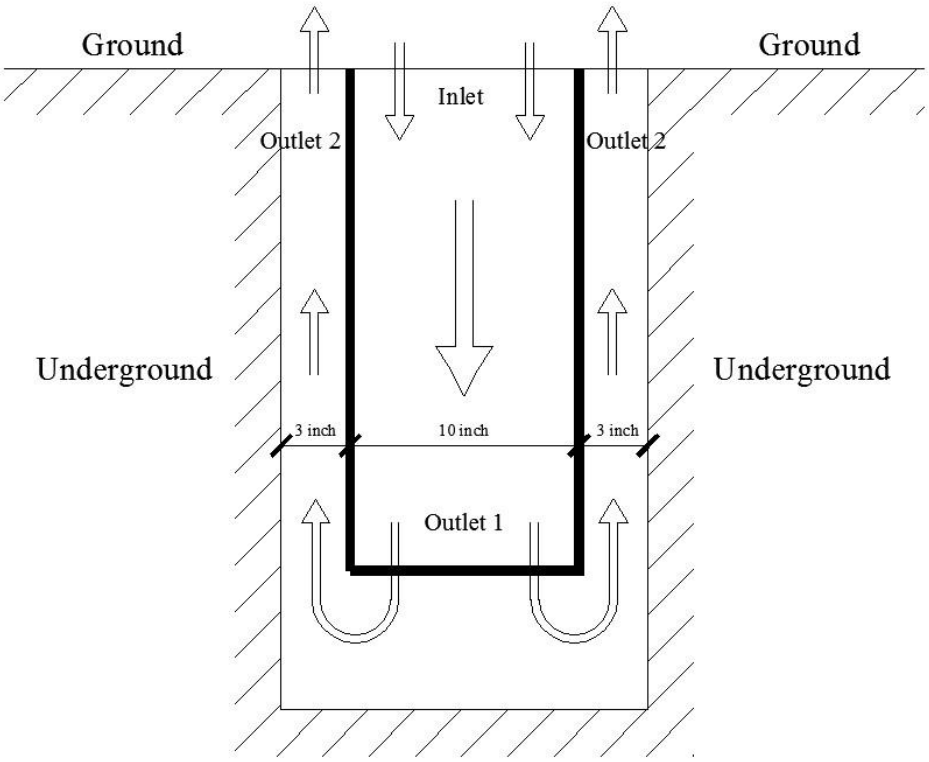


Fig. 4.1 Air Drilling Application

### 4.2 Boundary Conditions

As has been discussed above, the pressure at cold end outlet of the vortex tube bundle is 2.5MPa, thus the inlet pressure in the Fig. 4.1 is also 2.5MPa. The drill pipe is made of steel and the convection heat transfer rate is assumed to be 25 W/m • $k^{-1}$. The temperature of the subsurface rock increases approximately $1^{o}C$ per 33m increase in depth. The end of drill pipe is set as an interior outlet in the numerical simulation and the real outlet for the gas is at the ground level which is set to have the atmospheric pressure. Table 4.1 summarizes the boundary conditions used in the simulations:

Table 4.1 Boundary condition settings

| | |
|---|---|
| Inlet-temperature | 272 K |
| Inlet-pressure | 2.5MPa |
| Outlet1 | Interior outlet |
| Outlet2-pressure | 0.1MPa |
| Inner wall material | Steel |
| Outer wall (rock) temperature increase | $1\ ^{o}C/33m$ |

### 4.3 Meshing

Assumption as the problem is axis-symmetric has been made. To speed up the computations, the dense mesh near the ends is allocated, and use sparse grids in the mid portion of the pipe (Fig. 4.2).

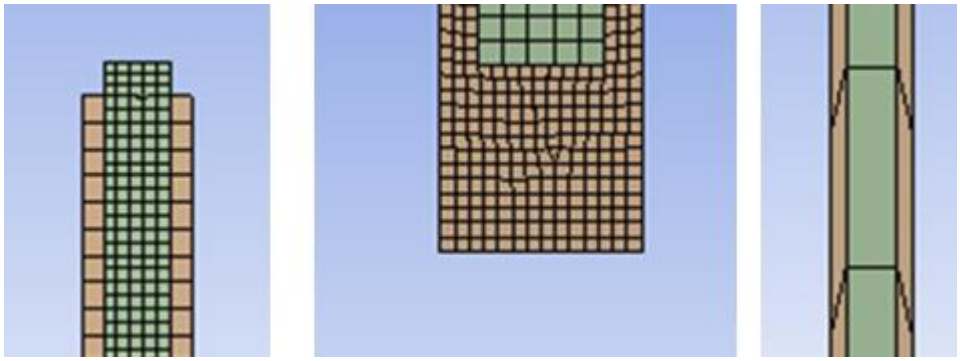

Fig. 4.2 Mesh method

Grid independence is also conducted, similar to the vortex tube simulations. A converging plot is given in Fig. 4.3.

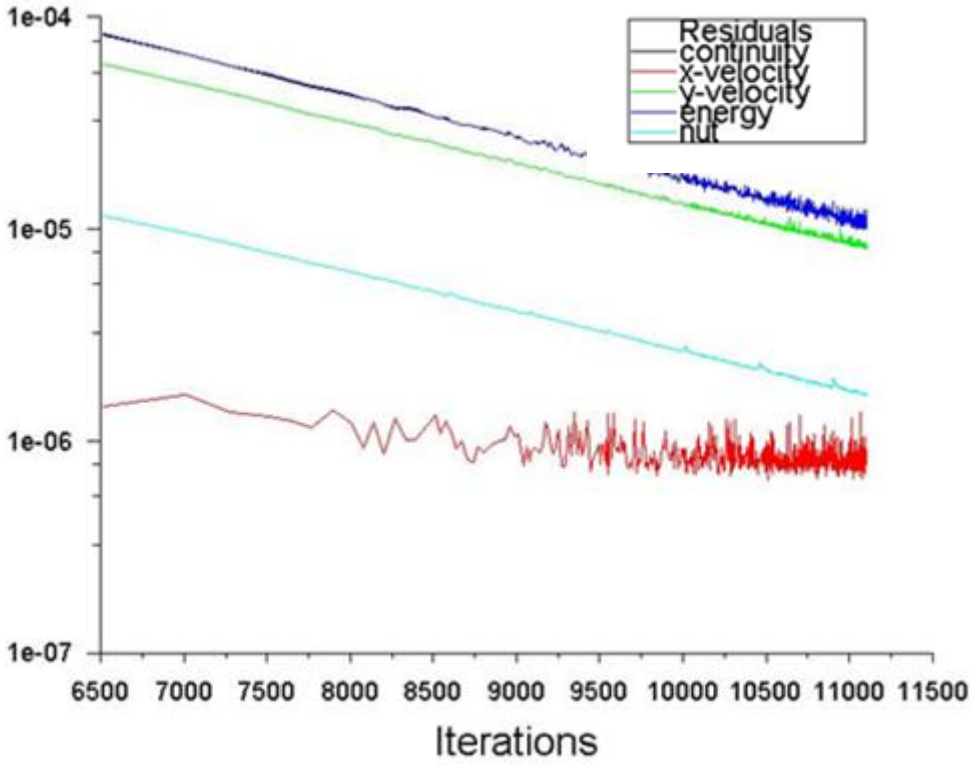


**Fig 4.3 Convergence study**

## 4.4 Results

Simulations for depths of 100m, 200m and 200m with a rock temperature

gradient of 4°C/33m (instead of 1°C/33m), have been performed. Simulations for depths greater than 500 m require extremely large number of grid points and it takes significantly longer time to compute. Fig. 4.4 shows the temperature change with depth in the drill pipe (red line) and the return air along the annulus (black line) for drilling to 100m. At the drilling head (100 m), the air temperature is 0 °C, an increase of 2 °C from the cold air entering the drill pipe on the surface.

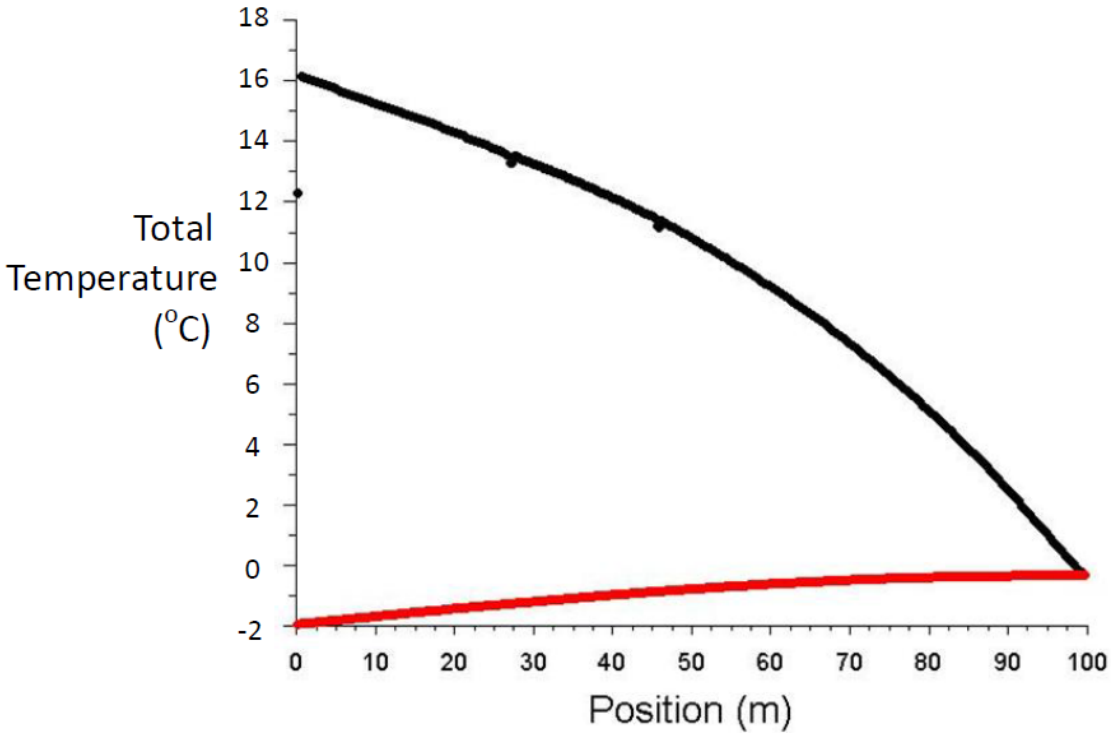


Fig. 4.4 Drilling to 100m depth.

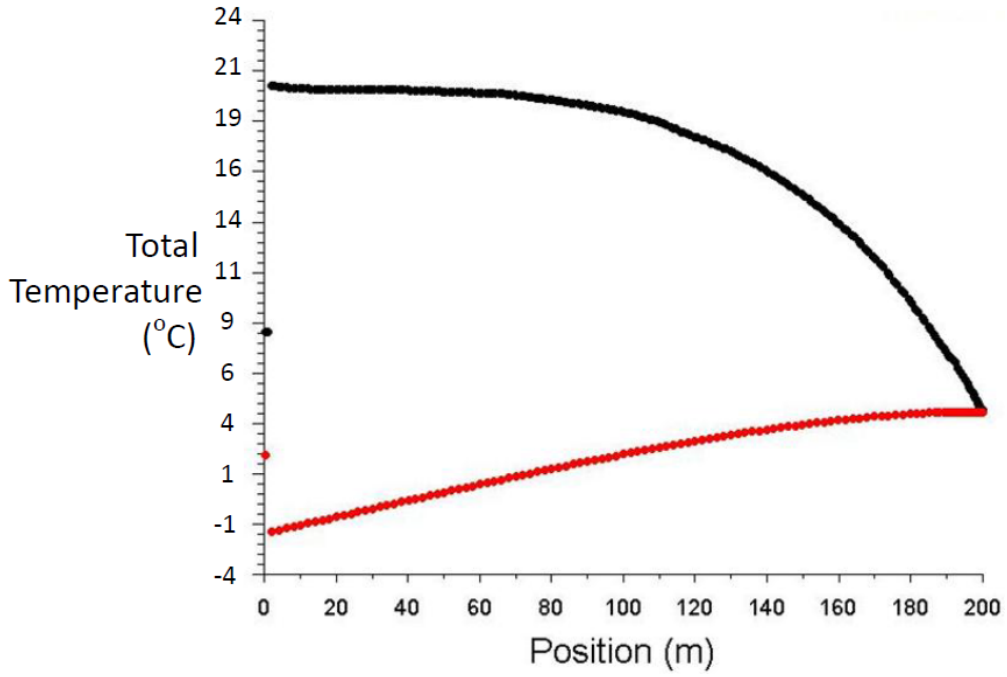


Fig. 4.5 Drilling to 200m depth.

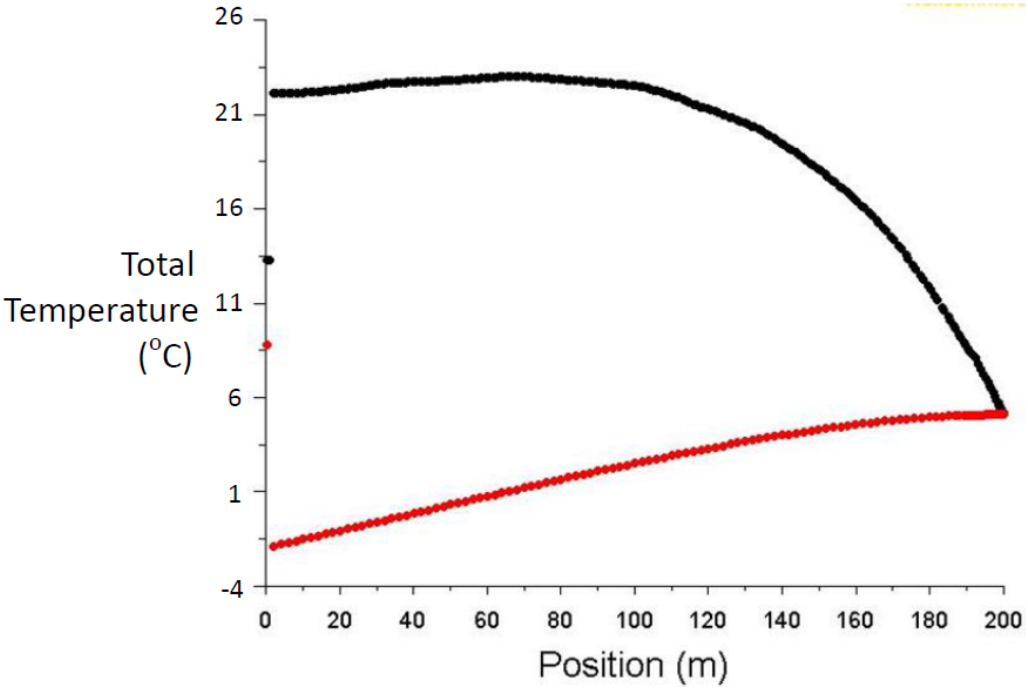


Fig. 4.6 Drilling to 100m depth with 4°C/33m vertical temperature gradient.

Similar calculation for drilling to 200m was also performed, with the temperature variation with depth given in Fig. 4.5. The air temperature at the drilling

head is about 3 $^{o}$C, an increase of 5$^{o}$C from the cold air entering the drill pipe on the surface.

A calculation for a much greater rock temperature gradient, 4$^{o}$C/33m instead of 1$^{o}$C/33m, is presented in Fig. 4.6 for drilling to 200 m depth. Even at this large rock temperature increase rate, the air at drilling head is at a relatively low temperature 5 $^{o}$C, an increase of 7 $^{o}$C from the cold air entering the drill pipe on the surface.

These three examples show that the idea of using a vortex tube bundle is suitable for use in air drilling applications.

# CHAPTER 5

# CONCLUSIONS

A vortex tube can separate a compressible air into a hot and a cold air stream. It has a simple structure with no moving parts; it is easy to manufacture and assemble, and it is easy to operate with no maintenance required. Despite of its low energy efficiency, it has been widely used in many applications.

Using numerical simulations, this thesis explores the possibility of using a vortex tube bundle for application is drilling applications. The major findings of this study are:

(1) Inlet pressure is a key parameter for the vortex tube performance. Increasing the inlet pressure improves the energy separation effect in general. However, when the inlet pressure to the cold outlet pressure ratio becomes large, the rate of drop in the cold outlet temperature levels off. Furthermore, when this pressure ratio exceeds certain value so that shock waves appear, the temperature drop starts to decreases, corresponding to a transition from subsonic to supersonic flow at the tube inlet.

(2) An optimization of the temperature drop with geometric parameters has been performed starting from the original design, and a large scale optimized vortex tube providing the required performance is found. This optimized vortex tube is characterized by: Length of 798mm, the diameter of the tube of 57mm, the area of inlet of 378.45mm$^2$ with rectangular shape of width of 8.7mm and length of 43.5mm;

The radius at the hot end outlet of 25mm; and the radius at the cold end outlet of 14.25mm. With this design, the performance of the tube is given in Fig. 3.8 for various inlet pressures. An inlet air pressure of 8 MPa with 16 such tubes meets the requirement of the cold end flow-rate of 40kg/s, pressure of 2.5 MPa, with maximum temperature drop of 22$^{o}$C.

(3) Simulations using the cold end air from the bundle of vortex tubes for air drilling application have been performed for drilling depth of 100m, and 200m. The air temperature at the drilling head can be maintained at 4-5 $^{o}$C.

## REFERENCES


[1] G.J. Ranque. Method and apparatus for obtaining from a fluid under pressure two currents of fluid at different temperatures. United States Patent 1952281, March 27, 1936.

[2] G.J. Ranque. Experiment on expansion in a vortex tube with simultaneous expansion of hot air and cold air. Le Journal de Physics et Le Radium (Paris),1933, v.4.1128.

[3] R Hilsch. The use of the expansion of gases ina centrifugal field as cooling process [J]. The review of scientific instruments, 1947, 8(2): 108-113.

[4] Zhang W.Z. The application of vortex tube in industrial field.

[5] Hu H.T. Air refrigeration cycle characteristics and a new type of refrigeration equipment research. Energy Saving. 2001(12):13-15.

[6] Sun. G.H. Refrigeration theory and application of vortex tube. 1988

[7] Cao Y. Development and summary of vortex tube research[J]. Cooling Engineering. 2001(6):1-5.

[8] Huang F.G. Application and practice of vortex tube refrigeration. 1992(3):49-53.

[9] Ding Y.G. Application of vortex tube. Coolin Engineering. 2004(1)

[10] Sha Q.Y. New skill of gas handling. 1994.

[11] Fulton C D. Ranque's tube. ASRE Refrigeration Engineering, 1950, 58(5): 473-479.

[12] Van Deemter J S. On the theory of the Ranque-Hilsch cool effect. Applied scientific Research (Series A), 1952,3(3): 174-196.

[13] J E Lay. An experimental and analytical study of vortex-flow temperature separation by superposition of spiral and axial flows. Transaction of the ASME. Journal of heat transfer, 1959, 8:213-223.

[14] Stephan K, at el. An investigation of energy separation in a vortex tube. International Journal of Heat and Mass Transfer, 1983, 36(3): 341-348.

[15] R.G. Deissler and M Perlmutter. Analysis of the flow and energy separation in a turbulent vortex. International Journal of Heat and Tranfer, 1960: 173-191.

[16] K Stephan, S Lin, M Durst, D Seher. A similarity relation for energy separation in a vortex tube. International Journal of Heat and Mass Transfer, 1984: 911-920.

[17] George W Scheper. Then vortex tube: internal flow date and a heat transfer theory. Refrigeration engineering, 1951, October: 985-989.

[18] Gulyaev A L. The Ranque effect at low temperatures. International Chemical Engineering, 1966,6(2):461-466.

[19] T T Cockerill. Thermodynamics and fluid mechanics of Ranque-Hislch vortex tube:[Mscthesis]. University Cambridge, 1998.

[20] J P Hartnett. Experimental study of the velocity and temperature calibration in a high velocity vortex tube flow. Transaction of the ASME, 1957, May: 751-758.

[21] C U Linderstrom-Lang. The three-dimensional distributions of tangential velocity and total-temperature in vortex tube. Journal of Fluid of Mechanics, 1971, 45: 161-187.

[22] Kurosaka M K. Acoustic streaming in swirling flow and the Ranque-Hilsch effect. Journal of Fluid Mechanics, 1982, 124: 139-172.

[23] E.R.G Eckert. Energy separation in fluid streams. International Communications in heat and mass transfer, 1989,13(2):127-143.

[24] B Ahlbor, S Groves. Secondary flow in vortex tube. Fluid Dyn. Res, 1997:73-86.

[25] B Ahlborn. The heat pump in a vortex tube. Non-Equilih. Thermodyn, 1998(2): 159-165.

[26] B Ahlborn. The vortex tube as a classic thermodynamics refrigeration cycle. Journal of Applied Physics, 2000,88(6): 3646-3653.

[27] B Ahlborn, Keller J.U, Staudt R, Treitz G, Rebhan E. Limits of temperature separation in a vortex tube. Journal of Applied Physics, 1994,27:480-488.

[28] Numerical investigation of gas species and energy separation in the Ranque-Hilsch vortex tube using real gas model

[29] M.H. Saidi, M.S. Vlipour, Experimental Modeling of Vortex Tube Refrigerator. Applied Thermal Engineering, 2003,23:1971-1980.

[30] Song. Jiang. Gao et al. experimental research on vortex board refrigeration effect. Cooling Engineering, 2006, (2).

[31] Hu. Experimental research on small flow rate vortex tube hot end humidification refrigeration system. Refrigeration Tech. 2002(2).

[32] Heishichiro Takahama. Studies on vortex tube. Japan Society of Mechanical Engineers, 1965,8(31);

[33] Parulekar B.B Performance of short vortex tubes. Journal of Institution of

Engineers(India), 1960(8): 161-164.

[34] Upendra Behera, P.J. Paul, S Kasthuriengan. CFD analysis and experimental investigations toward optimizing the parameter of Ranque-Hilsch vortex tubee[J]. Heat and mass transfer, 2005.

[35] Metenin V.An investigation into counter-flow vortex tubes. International Chemical Engineering. 1964,4(3):464-466.

[36] Heishichiro Takahama, Hajime Yokosawa. Energy separation in vortex tubes with a divergent chamber. Transaction of the ASME Journal of Heat transfer, 1981,103(2):196-203.

[37] Tong Zhou. Turbulent calculation on application of 2nd order Renault stress. aircraft engine. 1995. (2)

[38] Zhongyue Huang. Improving the refrigeration effect of vortex tube. Refrigeration Tech, 2002, (1).

[39]Piralishvili S A, Polyaev V M. Flow and Thermodynamics Characteristics of Energy Separation in a double-circuit Vortex Tube-An Experimental investigation. Experimental Thermal and Fluid Science, 1996:399-410.

[40] Guillaume D W, Jolly J L.Demonstrating the achievement of lower temperatures with two-stage vortex tube. Review of Scientific Instrument, 2001:3446-3448.

[41] Arbzov V A, Dubnischev Yu N, Lebrdev A V. Observation of large-scale structure in vortex tube by colored Foucault-hilbert visualization method. Third International Conference of Fluid Dynamics Measurement and its Applications. 1997:141-143.

[42] Marlyonvskii V S, Alekseseev V.P. Investigation of the vortex thermal separation effect for gases vapors. Soviet Physics, 1957,1:2232-2243.

[43] J Marshall. Effect of operation conditions, Physical size and Fluid characteristic on the gas separation performance of a Linderstrom-Lang vortex tube. Internation Journal of Heat and Mass Transfer. 1977,20(3):277-231

[44] Ueishichiro Takahama, et al. Performance characteristics of energy separation in a steam-operation vortex tube. International Journal Engineering Science, 1979, 17:735-744.

[45] Balmer R.T. Pressure Driven Ranque-Hiksch separation in liquids. Journal of Fluids engineering, 1998, 110:161-164.

[46] R.L. Collins, R.B. Lovelace. Experimental Study of Two-Phase Propane Expanded through the Ranque-Hilsch vortex tube. Journal of Heat Transfer. ASME, 1979, 101:300-305.

[47] Lancelot A Fekete. Vortex tube separator may solve weight/space limitations.

World Oil. 1986:40-44.

[48] A Williams. The cooling of methane with vortex tubes. Journal of Mechanical Engineering Science, 1971, 13(6):369-375.

[49] Thomas J Bruno. Laboratory application of vortex tube. Journal of Chemical Education, 1987, 64(11):987-988.

[50] Shou W.D. The application of vortex tube in refrigeration and gas industrial. 1990. (2): 48-51.

[51] Brock Hajdik, Manfred Lorey. Vortex tube can increase liquid hydrocarbon recovery at plant inlet. Oil and Gas Journal. 1997, 95(36):76-83.

[52] Webster. Analysis of the Hilsch Vortex tube. Refrigerating Engineering. 195:163-171.

[53] He Y.C. Comparison between three kinds of expansion equipment. Cryogenics and Superconductivity

[54] Aljuwayhel N.F. Nellis G.F. Parametric and internal study of the vortex tube using a CFD model. International Journal of Refrigeration. 2005,28:442-450.

[55] Bramo, A.R., Pourmahmoud, N., A Numerical Study on The Effect of Length to Diameter Ratio and Stagnation Point on The Performance of Counter Flow Vortex Tube, Aust. J. Basic and Appl. Sci., 4(2010), pp. 4943-4957

[56] Skye. Comparison of CFD analysis to empirical data in a commercial vortex tube.

[57] Effects of geometric parameters on the separated air flow temperature of a vortex tube for design optimization. Energy 37(2012) 154-160.

[58] Nader. Computational Fluid Dynamics Analysis of Helical Nozzles Effects on the Energy Separation in a Vortex Tube. Thermal Science. 2012, Vol. 16, No. 1, pp. 151-166

[59] A.P. Merkulov, Vikhrevoi Effekt I Ego Primenenie VTekhnike (Vortex Effect and Its Application in Technique),Mashinostroenie, Moscow, 1969.

[60] T. Dutta. Numerical investigation of gas species and energy separation in the Ranque-Hilsch vortex tube using real gas model. International Journal of Refrigeration 34(2011) 2118-2128.

[61] H.H Bruun. Experimental investigation of the energy separation in vortex tubes[J]. Journal mechanical engineering science, 1969, 11(6):567-582.

[62] Upendra Behera. CFD analysis and experimental investigations towards optimizing the parameters of Ranque-Hilsch vortex tube. International Journal of Heat and Mass Transfer. Volume 48, Issue 10, May 2005, Pages 1961-1973